Am J Physiol Gastrointest Liver Physiol 298: G107–G116, 2010.
First published October 29, 2009; doi:10.1152/ajpgi.00391.2009.

Kupffer cell activation is a causal factor for hepatic insulin resistance

Nicolas Lanthier,[1] Olivier Molendi-Coste,[1] Yves Horsmans,[1] Nico van Rooijen,[2] Patrice D. Cani,[3] and Isabelle A. Leclercq[1]

[1]*Laboratory of Gastroenterology, Université catholique de Louvain, Brussels, Belgium;* [2]*Department of Molecular Cell Biology, Vrije Universiteit Medical Center, Amsterdam, The Netherlands; and* [3]*Louvain Drug Research Institute, Unit of Pharmacokinetics, Metabolism, Nutrition and Toxicology, Université catholique de Louvain, Brussels, Belgium*

Submitted 23 September 2009; accepted in final form 22 October 2009

Lanthier N, Molendi-Coste O, Horsmans Y, van Rooijen N, Cani PD, Leclercq IA. Kupffer cell activation is a causal factor for hepatic insulin resistance. *Am J Physiol Gastrointest Liver Physiol* 298: G107–G116, 2010. First published October 29, 2009; doi:10.1152/ajpgi.00391.2009.—Recruited adipose tissue macrophages contribute to chronic and low-grade inflammation causing insulin resistance in obesity. Similarly, we hypothesized here that Kupffer cells, the hepatic resident macrophages, play a pathogenic role in hepatic insulin resistance induced by a high-fat diet. Mice were fed a normal diet or high-fat diet for 3 days. Kupffer cell activation was evaluated by immunohistochemistry and quantitative RT-PCR. Insulin sensitivity was assessed in vivo by hyperinsulinemic-euglycemic clamp and insulin-activated signaling was investigated by Western blot. Liposome-encapsulated clodronate was injected intravenously to deplete macrophages prior to a short-term exposure to high-fat diet. Here, we characterized a short-term high-fat diet model in mice and demonstrated early hepatic insulin resistance and steatosis concurrent with Kupffer cell activation. We demonstrated that selective Kupffer cell depletion obtained by intravenous clodronate, without affecting adipose tissue macrophages, was sufficient to enhance insulin-dependent insulin signaling and significantly improve hepatic insulin sensitivity in vivo in this short-term high-fat diet model. Our study clearly shows that hepatic macrophage response participates to the onset of high-fat diet-induced hepatic insulin resistance and may therefore represent an attractive target for prevention and treatment of diet- and obesity-induced insulin resistance.

macrophage; liver; steatosis; liposomes; high-fat diet

NONALCOHOLIC FATTY LIVER DISEASE (NAFLD) becomes in our sedentary societies the most common cause of chronic liver disease (1). It is associated with obesity and insulin resistance and is now considered as the hepatic manifestation of the metabolic syndrome (50, 51). Fat accumulation in the liver is associated with higher cardiovascular mortality, in addition to liver-related cause of death, such as progression to nonalcoholic steatohepatitis and fibrosis or sensitization to other hepatic injuries (1, 49). Hepatic insulin resistance refers to inadequate insulin-dependent suppression of hepatic glucose production (HGP) and plays a pivotal role in the development of hyperglycemia and evolution toward type 2 diabetes (17, 30). Hepatic insulin resistance is the hallmark of NAFLD (31, 46). Hepatic lipid overload, lipid metabolites, and proinflammatory mediators have all been shown to alter hepatic insulin sensitivity in vivo and in vitro (38, 47). Knowing the role of diabetes in the progression of hepatic inflammation and fibrosis (7, 14, 18) and the potential benefits of improving insulin resistance in decreasing risk of cardiovascular related death, targeting hepatic insulin resistance may represent a new therapeutic approach for NAFLD and related diseases.

Several studies have linked insulin resistance to systemic inflammation (11, 45). Anti-inflammatory aspirin is long known to lower blood glucose (13). Mice lacking the proinflammatory cytokine TNF are protected from insulin resistance induced by chronic high-fat feeding (10). Conversely, activation of proinflammatory JNK or IκB kinase-β pathways have been found to promote obesity-induced insulin resistance (6, 12). Fat-overloaded adipocyte, because it produces numerous chemokines and (adipo)cytokines affecting immunity and inflammation, was seen as an important player in this process. More recently, attention has been brought to bone marrow-derived macrophages recruited to obese visceral adipose tissue (28, 56, 59) as a source for inflammatory factors altering metabolic functions of adipocytes and causing insulin resistance both locally and in distant organs. Accordingly, F4/80^+CD11b^+CD11c^+ M1 adipose tissue macrophages (ATM) increase in number in obese adipose tissue (28, 34) and suppression of such inflammation improves insulin sensitivity and dissociates adiposity from insulin resistance (15, 37, 42, 48, 55). Genetic manipulations of IκB kinase-β or JNK signaling in myeloid lineage affect systemic metabolic regulations (48, 58, 61). Collectively, data available to date show that, without a myeloid cell-driven inflammatory component, obesity itself does not cause insulin resistance.

Recent data suggest that hepatic steatosis resulting from high-fat feeding is associated with activation of Kupffer cells (KC), the hepatic resident macrophages (2, 57). A causal link between KC activation and hepatic insulin resistance has been suggested (33, 44) but never convincingly experimentally addressed.

The aim of our study is to characterize hepatic inflammation induced by high-fat feeding and determine whether such inflammation participate to the initiation of hepatic insulin resistance. We used a short-term high-fat diet (HFD) model in mice and demonstrated early hepatic macrophage activation associated with hepatic insulin resistance and steatosis. We addressed the role of activated resident macrophages in the liver (KC) on hepatic insulin sensitivity using experimental macrophage depletion obtained by intravenous injections of liposome-encapsulated clodronate (53, 60).

MATERIALS AND METHODS

Animals, diets, and treatment. Five-week-old male C57BL/6J (Janvier, Le Genest-Saint-Isle, France) mice were fed for 3 days a HFD in which 60% of calories are derived from fat (D12492 from Research Diets, New Brunswick) or a standard rodent chow (10% of calories from fat, Carfil Quality, Oud-Turnhout, Belgium) referred to as normal diet (ND). The animals were handled according to the guide-

Address for reprint requests and other correspondence: I. Leclercq, Laboratoire de Gastro-entérologie, Université catholique de Louvain, GAEN 53/79, Ave. Mounier, 53, B-1200 Brussels, Belgium (e-mail: isabelle.leclercq@uclouvain.be).

lines for humane care for laboratory animals established by the Université catholique de Louvain in accordance with European Union Regulation. The study protocol was approved by the local ethics committee. At the time of euthanasia, under anesthesia, mice received 5 U insulin (Actrapid, Novo Nordisk, Bagsvaerd, Denmark) or an equal volume of PBS into the portal vein to analyze the intrahepatic response to insulin. The liver was removed 1 min after the injection, and epididymal and subcutaneous adipose tissues and right quadriceps were dissected and weighed. Portions of tissue were immersed in formalin 4% or frozen in optimal cutting temperature medium for histological studies; the remaining tissue was snap frozen in liquid nitrogen and kept at −80°C until analyses. To deplete macrophages, 100 μl/10 g body wt of 1 mg/ml liposome-encapsulated clodronate, or liposome-encapsulated PBS, or an equal volume of NaCl 0.9% were injected to mice intravenously (iv) via the retroorbital plexus, 24 h prior to the administration of the HFD. In a parallel experiment, mice received NaCl 0.9%, liposome-encapsulated PBS, or liposome-encapsulated clodronate by intraperitoneal injection. Clodronate (a gift from Roche Diagnostics, Mannheim, Germany) was encapsulated into liposomes as described previously (53). Clodronate and liposomes by themselves are not toxic. Liposomes, taken up by phagocytic cells (macrophages), are disrupted by lysosomal enzymes. This provokes the intracellular release of clodronate, causing apoptotic cell death of macrophage (54). Analyses were performed on eight animals per group.

Hyperinsulinemic-euglycemic clamp study. Femoral iv catheter was implanted 7 days before clamp studies (4). HGP and whole body glucose turnover (TO) were evaluated by the hyperinsulinemic-euglycemic clamp technique (8, 16), conducted at 11:00 AM after a 5-h fast with a continuous infusion of 2.5 $mU \cdot kg^{-1} \cdot min^{-1}$ human insulin (Actrapid) coupled with [3-^{3}H]glucose (0.33 μCi, PerkinElmer, Boston, MA). Tail blood glycemia was obtained at *time 0* and every 10 min thereafter to adjust a variable 20% glucose infusion rate (GIR) to maintain euglycemia (90–110 mg/dl). When steady-state was obtained (±90 min), blood samples (5 μl) were collected every 10 min for 1 h for estimation of plasma glucose specific activity. At steady state, the rate of glucose appearance (Ra) measured as = [3-^{3}H]GIR/glucose specific activity equals the rate of peripheral glucose disposal (Rd) or TO (4, 5). In basal conditions, the rate of HGP ($mg \cdot kg^{-1} \cdot min^{-1}$) equals Ra. In insulin stimulated conditions (2,5 $mU \cdot kg^{-1} \cdot min^{-1}$), HGP was obtained by subtracting the GIR ($mg \cdot kg^{-1} \cdot min^{-1}$) to the Rd previously calculated: HGP (Ra) = Rd − GIR. Analyses were performed on five to eight animals per group.

Biochemical analyses. Blood glucose concentrations were determined with a glucose monitor (Accu-chek, Aviva, Roche) and plasma insulin levels by using an enzyme-linked immunoassay (Mercodia, Uppsala, Sweden). Total liver lipids were extracted with methanol and chloroform and quantified by the vanillin-phosphoric acid reaction (22).

Histology, immunohistochemistry, and immunofluorescence. Hematoxylin and eosin staining were used for routine histological evaluation. Immunohistochemical detection of F4/80 was performed on paraffin-embedded sections treated with proteinase K by using a primary rat anti-mouse F4/80 monoclonal Ab (1/200, Serotec, Oxford, UK), a rabbit anti-rat immunoglobulin (1/200, Dako, Glostrup, Denmark), and then a goat anti-rabbit streptavidin horseradish peroxidase-conjugated Ab (En Vision, Dako). The peroxidase activity was revealed with diaminobenzidine and slides were counterstained with hematoxylin. Morphometrical quantification of the surface stained was performed on microphotographs (×20) taken from two random sections per liver (n = 6 per group) by use of the Axiovision 4.6 image analysis software (Carl Zeiss, Goentingen, Germany) and expressed as percentage of total area as previously described (52). CD68, C11b, and CD11c-positive cells were detected on cryosections (5 μm thick) by using a monoclonal rat anti-mouse CD68 (1/300, Serotec), a monoclonal rat anti-mouse CD11b (1/100, Developmental Studies Hybridoma Bank, Iowa City, IA) or a monoclonal hamster anti-mouse CD11c Ab (1/50, Serotec). For double immunofluorescence, the same primary Abs were used as well as a polyclonal F4/80 rabbit anti-mouse Ab (1/500, Santa Cruz, CA) when indicated. Secondary Abs were anti-rat/AlexaFluor 594, anti-rabbit/AlexaFluor 488, or anti-hamster/AlexaFluor 488 (dilution 1/1,000, Invitrogen, Merelbeke, Belgium). Hoechst (dilution 1/10.000) was used to reveal the nuclei.

Protein studies: Western blotting. Liver and muscle homogenates were prepared as described elsewhere (23). Proteins (100 μg) were assayed by Western blotting using the Abs and conditions listed in Supplemental Table S1. The immunoreactivity was detected with a horseradish peroxidase-conjugated secondary Ab (1/10,000) and chemiluminescence (PerkinElmer). One membrane was sequentially probed with the Ab against the total protein, the phosphoprotein, and HSP90 to control for protein loading. The quantification of immunereactive proteins was obtained by densitometry using the Gel DocTM XR System 170–8,170 device and software (Bio-Rad). The levels of immunoreactivity relative to the invariant control are reported as arbitrary densitometry units.

RNA extraction, reverse transcription, and quantitative PCR. Total RNA was extracted from frozen liver, subcutaneous or epididymal fat samples by using TRIpure Isolation Reagent (Roche Diagnostics Belgium, Vilvoorde, Belgium). cDNA synthesis and real-time PCR analysis were carried out as previously described (23). Primer pairs for transcripts of interest were designed using the Primer Express software (Applied Biosystems, Lennik, Belgium) and listed in Supplemental Table S2. RPL19 mRNA was chosen as an invariant standard. All experimental tissues and standard curve samples were run in duplicate in a 96-well reaction plate (MicroAmp Optical, Applied Biosystems). Results are expressed as fold expression relative to expression in the control group following the ΔΔCt method (26).

Statistical analysis. All the data are presented as means ± SD. Statistical analysis was performed by ANOVA for multiple groups comparison and Student's t-test for comparing two groups. When P was less than 0.05, differences were considered significant.

RESULTS

Short-term high-fat feeding induces obesity, adiposity, and liver steatosis. Compared with ND, a 3-day course of HFD induced body weight gain, increased adiposity, and increased relative liver weight (Table 1). On histological examination, lipid vacuoles were seen predominantly in the intermediate and periportal zones (Fig. 1*B*). Steatosis in HFD-fed animals was confirmed by a fourfold increase in hepatic lipid content (Table 1).

Short-term high-fat fed mice are insulin resistant, with the evidence of a specific hepatic insulin resistance. HFD-fed animals had increased fasting glucose levels with normal insulinemia (Table 1). Insulin sensitivity, assessed by the gold standard hyperinsulinemic euglycemic clamp technique, was reduced

Table 1. *Morphological, hepatic, and metabolic changes induced by a 3-day HFD*

	ND	HFD
Body weight gain, g	0.3±0.5	3.8±0.9*
Epididymal adipose tissue weight/ body weight, %	1.0±0.2	1.3±0.1*
Liver weight/body weight, %	5.6±0.3	6.4±0.5†
Hepatic lipid content, mg/100 mg liver	4.5±0.5	19.2±4.0*
Blood glucose, mg/dl	136.6±12.3	164.1±8.4†
Serum insulin, μg/l	1.2±0.9	1.3±0.3

Results are expressed as mean ± SD (n = 8 per group). Mice were fed a normal diet (ND) or a high-fat diet for 3 days (HFD). *$P < 0.001$ and †$P < 0.01$ in HFD vs. ND.

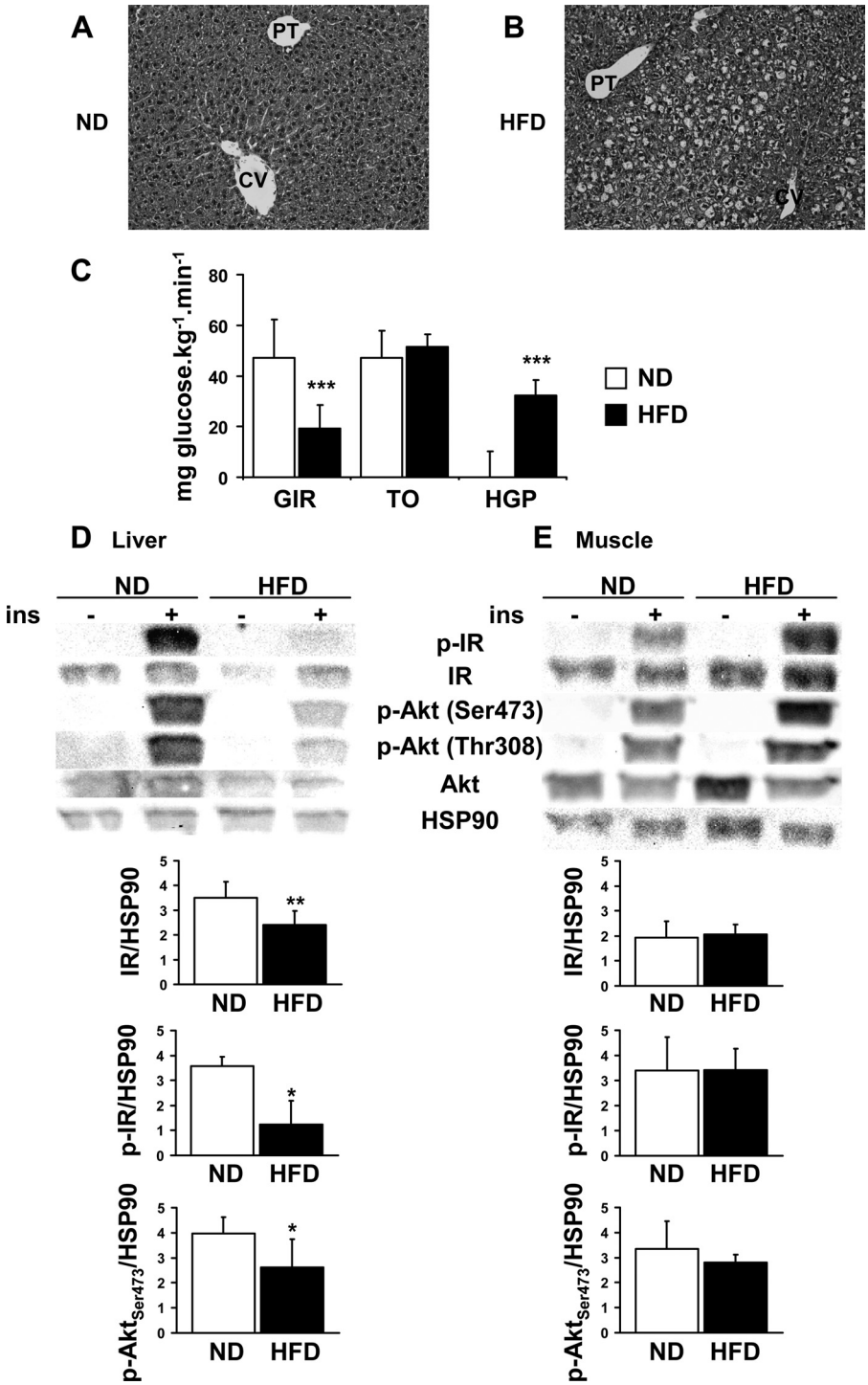

Fig. 1. Short-term high-fat diet (HFD)-fed mice develop steatosis and hepatic insulin resistance. *A* and *B*: representative photomicrographs of hematoxylin and eosin-stained sections of livers from mice fed the normal diet (ND; *A*) and the HFD (*B*) for 3 days. Original magnification ×20. PT, portal tract; CV, centrilobular vein. *C*: glucose infusion rate (GIR), glucose turnover (TO), and hepatic glucose production (HGP) during hyperinsulinemic-euglycemic clamps in mice fed the ND or the HFD for 3 days. Hepatic (*D*) and muscle protein expression (*E*) and phosphorylation of the insulin receptor (IR) and Akt evaluated by Western blot analysis in mice fed the ND or the HFD for 3 days, 1 min after the portal injection of insulin (+ins) or PBS. Representative blots and graphs representing the ratio of the (insulin-stimulated phospho-) protein of interest on HSP90 as measured by densitometry analysis (n = 4/group). Data are expressed as means ± SD. $^{*}P < 0.05$, $^{**}P < 0.01$, and $^{***}P < 0.001$ in HFD vs. ND.

in the HFD group as demonstrated by a lower GIR required to maintain euglycemia (Fig. 1*C*). This was owed to a marked impairment of insulin-dependent inhibition of HGP, a parameter completely inhibited in controls. In contrast, whole body glucose uptake (or TO) was not different in HFD and ND (Fig. 1*C*).

In the liver, HFD decreased the expression of insulin receptor (IR) but did not induce significant changes in Akt protein levels (Fig. 1*D*). Insulin-stimulated phosphorylation of IR and Akt (on Ser473 and Thr308) was significantly lower in HFD compared with ND livers (Fig. 1*D*). These changes were not observed in the muscle, where expression of IR, Akt and insulin-stimulated p-IR and p-Akt were similar in HFD and ND groups (Fig. 1*E*).

Collectively, those data demonstrate a marked hepatic insulin resistance but normal peripheral insulin sensitivity in mice fed the HFD for 3 days.

HFD induces an early activation of hepatic and ATM. Compared with ND livers (Fig. 2*A*), enlarged F4/80-positive mature tissue resident macrophages were preferentially found in the vicinity of lipid-loaded hepatocytes in HFD livers (Fig.

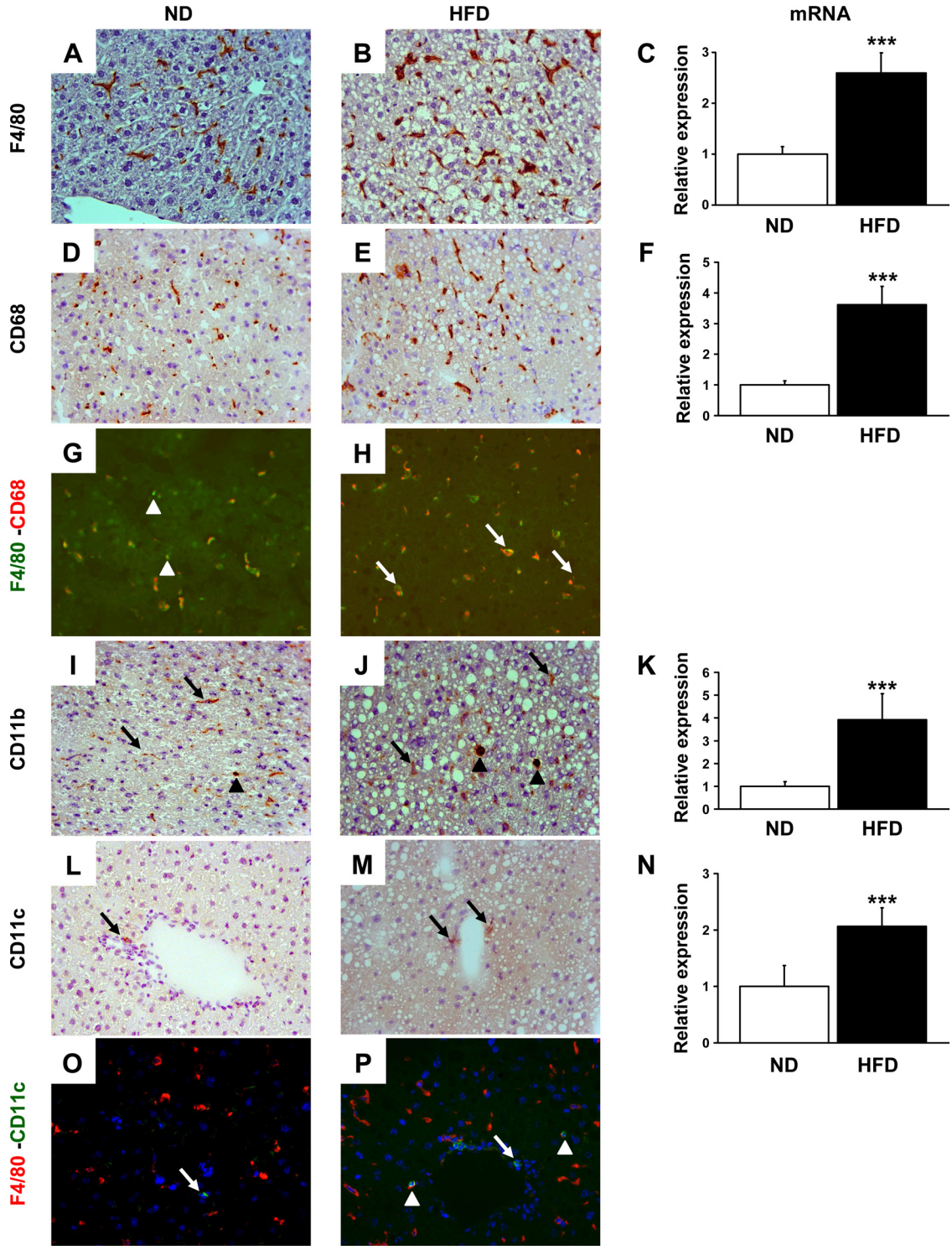

Fig. 2. HFD activates Kupffer cells. Liver sections from mice fed the ND (*A*, *D*, *G*, *I*, *L*, *O*) and the HFD (*B*, *E*, *H*, *J*, *M*, *P*) immunoassayed with antibodies against F4/80 (*A* and *B*), CD68 (*D* and *E*), F4/80 and CD68 (*G* and *H*; arrows point to double-positive cells), CD11b (*I* and *J*), CD11c (*L* and *M*), F4/80 and CD11c (*O* and *P*). CD11b staining revealed faintly stained, elongated cells (arrows) reminiscent of F4/80$^+$ cells and strongly positive round cells (arrowheads; *I* and *J*). CD11c$^+$ cells were rare and predominantly located around the portal tract (*L* and *M*, arrows). Some F4/80$^+$ (red) and CD11c$^+$ (green) double-positive cells (arrowheads) were found only in HFD livers (*P*). Original magnification ×40. mRNA for macrophage markers assessed by real-time PCR (*C*, *F*, *K*, *N*) in ND and HFD livers ($n = 8$ per group). Data are expressed as relative means ± SD to ND values arbitrarily set at 1. ***$P < 0.001$ in HFD vs. ND.

2*B*). This was confirmed by morphometrical analysis (F4/80-stained surface of 2.31 ± 0.85% in HFD livers vs. 0.85 ± 0.21% in controls, $P = 0.005$) and by the upregulation of F4/80 mRNA (Fig. 2*C*). An increased number of cells expressing the CD68/macrosialin, a transmembrane protein expressed by activated tissue macrophages (39), was found in the HFD livers compared with controls (Fig. 2, *D* and *E*) and confirmed by upregulation of hepatic CD68 mRNA (Fig. 2*F*). Immunofluo-

Table 2. *Effect of clodronate on hepatic inflammation-associated markers in HFD-fed mice*

	ND	HFD	CLO + HFD
TLR2 mRNA	1±0.10	1.72±0.48†	1.27±0.32
TLR4 mRNA	1±0.17	1.47±0.21*	0.65±0.11‡
CD14 mRNA	1±0.21	1.61±0.47†	0.43±0.26‡
TNF mRNA	1±0.39	2.08±0.55*	0.76±0.51§

mRNA expression of hepatic inflammatory genes assessed by RT-PCR, with expression in normal diet (ND) arbitrarily set at 1. Data are expressed as mean ± SD for $n = 8$ per group. *$P < 0.001$ and †$P < 0.01$ in HFD group vs. ND. ‡$P < 0.001$ and §$P < 0.01$ in clodronate-treated high-fat fed mice (CLO + HFD) vs. HFD.

rescence double staining revealed that, in control livers, a small proportion of F4/80-positive macrophages also expressed CD68 (Fig. 2*G*). Under HFD, the proportion of F4/80 to CD68 double-positive cells increased (Fig. 2*H*), supporting that hepatic macrophages are activated. CD11b/MAC-1 is classically expressed by granulocytes, monocytes, NK cells, and tissue macrophages (24). Two distinct liver populations of $CD11b^+$ cells were detected: elongated and faintly stained cells morphologically and topologically reminiscent of tissue macrophages, and a population of round cells compatible with neutrophils or monocytes (Fig. 2*I*, arrows and arrowheads, respectively). Under HFD, the population of CD11b-positive cells appeared increased (Fig. 2*J*). The mRNA analysis showed an approximately fourfold upregulation of CD11b (Fig. 2*K*). CD11c is an integrin mainly expressed by dendritic cells and by some macrophages (27). CD11c-positive cells were rare and preferentially located around the portal tract (Fig. 2*L*) in the normal liver. Upon HFD, slightly more numerous CD11c-positive cells, remaining located in the periportal zone (Fig. 2*M*), were seen together with an approximately twofold increased in CD11c mRNA (Fig. 2*N*). Double immunostaining demonstrated that only a minority of F4/80-positive macrophages were CD11c positive in HFD livers (Fig. 2*P*). These were apparently absent in controls (Fig. 2*O*). In addition to phenotypic changes in hepatic macrophages, HFD also significantly induced TNF, TLR2, TLR4, and CD14 mRNA expression, considered as markers of inflammation (Table 2).

In the adipose tissue, whether epididymal or subcutaneous, no apparent inflammation was detected by (immuno)histochemical techniques (Fig. 3, *A* and *B*), contrasting with adipose tissue inflammation classically described in chronic HFD and obesity models (28, 56, 59). Nevertheless, a 3-day HFD increased F4/80, CD68, and CD11b mRNA levels by twofold (Fig. 3, *C–E*) in the epididymal adipose tissue, whereas CD11c mRNA remained unchanged (Fig. 3*F*). Those changes were not seen in the subcutaneous fat pads (not shown). Our data thus support the activation of ATM in intra-abdominal depots in our model despite the apparent absence of macrophage recruitment.

Selective KC depletion ameliorates hepatic insulin sensitivity. The injection of PBS-loaded liposomes to HFD-fed mice had no effect on macrophage populations in the liver (Fig. 4, *H–J*). By contrast, the injection of liposome-encapsulated clodronate

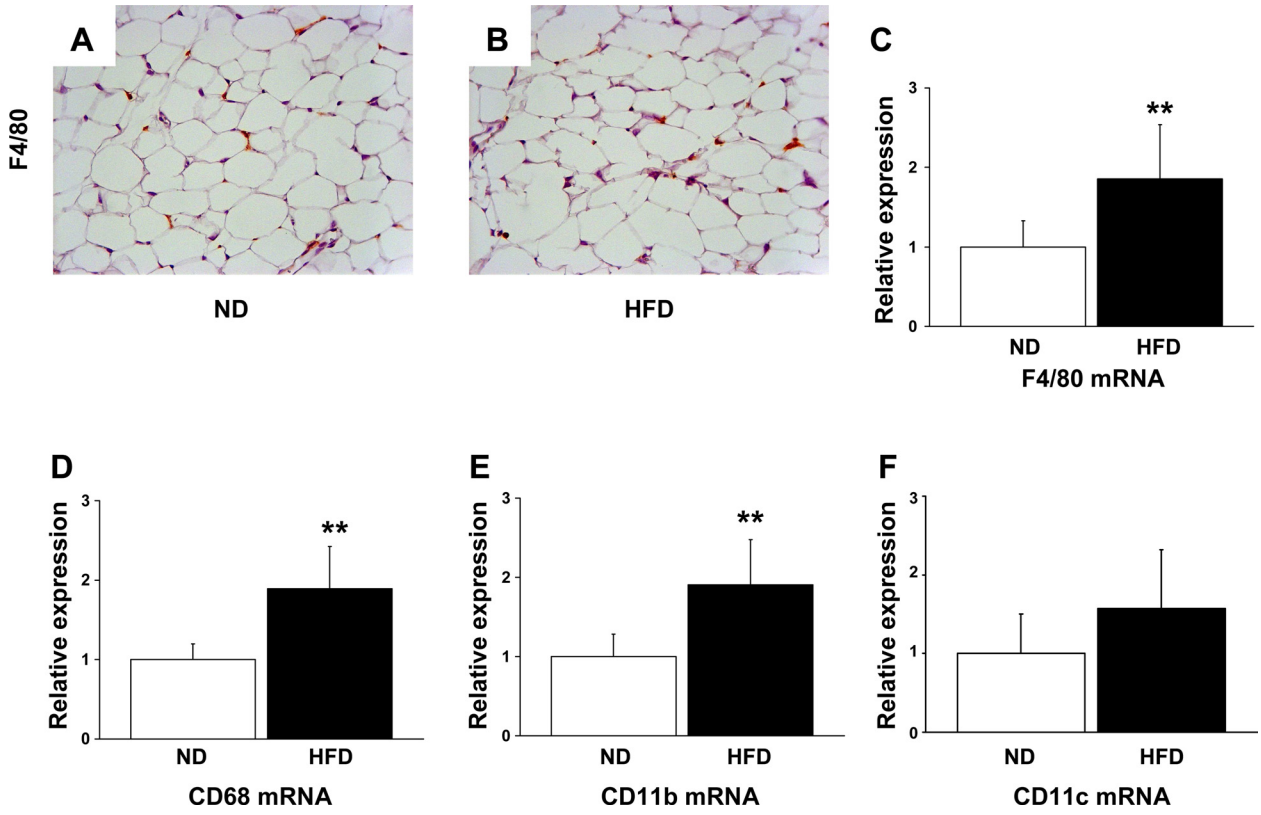

Fig. 3. Effects of a short-term HFD on adipose tissue expression of inflammatory markers. Immunohistochemical detection of the macrophage-specific antigen F4/80 in epididymal adipose tissue from mice fed the ND (*A*) or the HFD (*B*) for 3 days. Original magnification ×40. *C–F*: epididymal adipose tissue mRNA expression of inflammatory markers. Results ($n = 8$ per group) are expressed as means ± SD of fold expression compared with values in untreated ND animals arbitrarily set at 1. **$P < 0.01$ in HFD vs. ND.

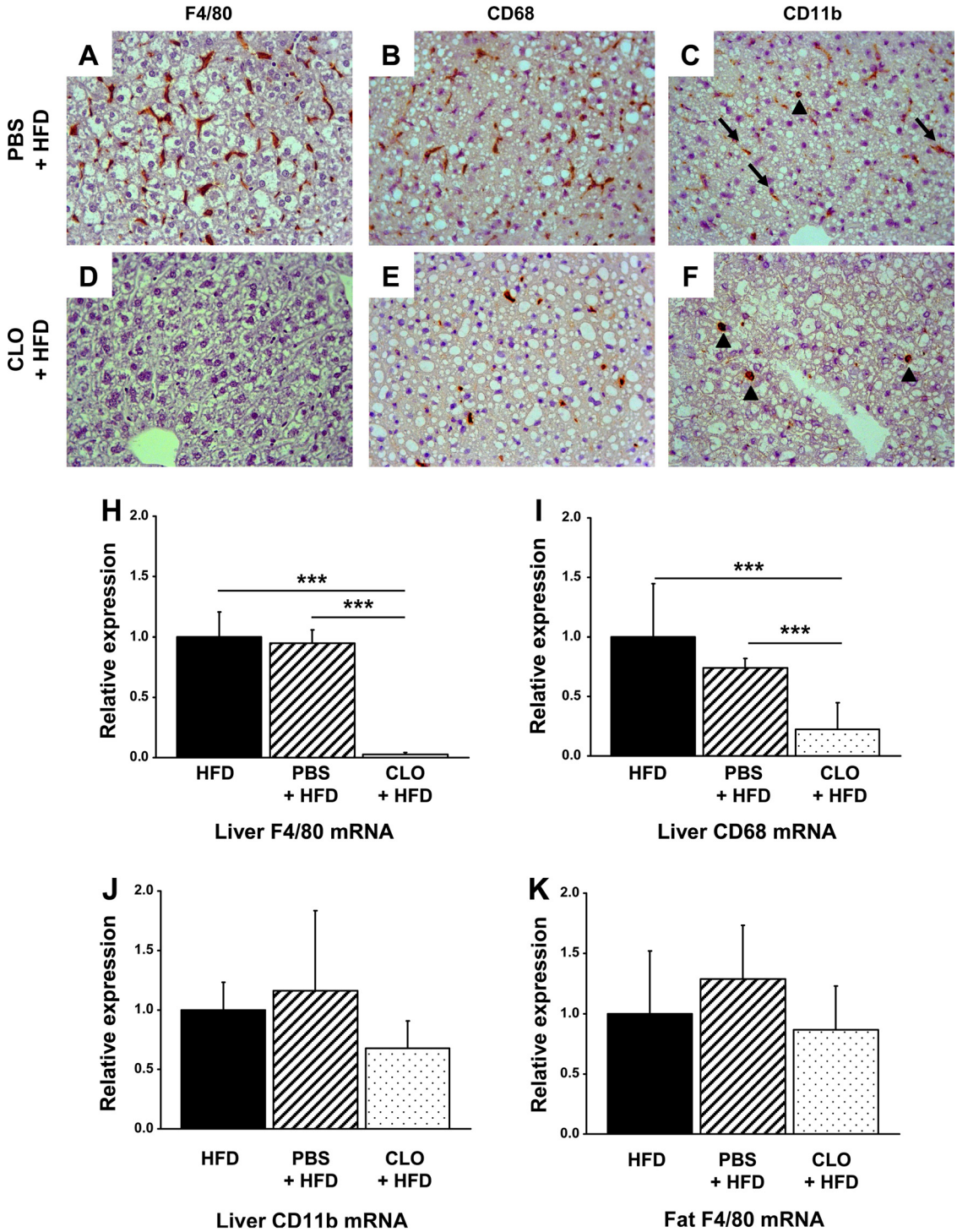

Fig. 4. Injection of liposome-encapsulated clodronate depletes Kupffer cells without affecting adipose tissue macrophages. F4/80 (*A* and *D*), CD68 (*B* and *E*), and CD11b (*C* and *F*) immunostaining on liver sections from mice fed the HFD with intravenous (iv) injection of PBS or clodronate loaded liposomes (PBS + HFD or CLO + HFD, respectively). Clodronate injection depleted F4/80, CD68, and CD11b (arrows)-positive cells with KC morphology (*D–F*); meanwhile a marginal population of round CD11b-positive cells (arrowheads) increased in the liver lobule (*F*). Immunohistochemistry on paraffin sections (F4/80) or frozen sections (CD68 and CD11b), brown staining. Original magnification ×40. Effects of iv liposome-encapsulated PBS (PBS + HFD) or clodronate injection (CLO + HFD) on liver (*H–J*) and epididymal adipose tissue (*K*) mRNA expression of macrophage markers. Results ($n = 8$ per group) are expressed as means ± SD of fold expression compared with untreated ND animal values arbitrarily set at 1. ***$P < 0.001$.

markedly and significantly depleted the liver of its F4/80, CD68, and CD11b-positive macrophages (Fig. 4, *A–F*). This was also assessed by a blunting in F4/80 and CD68 transcript expression (Fig. 4, *H–I*) whereas CD11b mRNA levels remained stable (Fig. 4*J*), reflecting the increased in nonmacrophage round CD11b-positive cells (Fig. 4*F*, arrowheads), consistent with the recruitment of blood monocyte precursors described by others (60). Hepatic CD11c mRNA remained

stable in the clodronate-treated HFD group (not shown). Paralleling macrophage depletion, clodronate injection was associated with a significant decrease in hepatic TNF, TLR4, and CD14 mRNA levels (Table 2).

PCR analysis demonstrated that clodronate liposomes did not affect inflammatory cell activity in the adipose tissue (Fig. 4*K*). Indeed, such liposomes, being unable to cross vascular barriers, are readily taken up by phagocytic cells in the reticuloendothelial system (53).

Fasting blood glucose, serum insulin levels, hepatic lipid content and body weight gain were not different whether HFD animals received or not PBS or clodronate whereas epididymal fat weight was lower in the clodronate treated group compared with others HFD groups (Table 3).

During clamp experiments, the GIR needed to maintain euglycemia significantly increased and insulin-dependent inhibition of HGP was significantly ameliorated in clodronate-treated animals compared with both PBS-treated and untreated HFD animals (Fig. 5*A*). At the level of insulin signaling, the specific depletion of hepatic macrophages did not improve IR phosphorylation whereas it significantly increased the phosphorylation of Akt in HFD livers (Fig. 5*B*).

DISCUSSION

In this study, we characterized a short-term HFD regimen in mice and used simultaneous ablation of KC through injection of liposome-encapsulated clodronate to demonstrate the role of hepatic macrophages in modulating hepatic insulin sensitivity.

Consistent with previous reports in rats (17, 43), feeding mice a HFD for 3 days provoked a significant body weight gain, steatosis, and selective hepatic insulin resistance, proved in vivo by hyperinsulinemic-euglycemic clamp technique and confirmed by defects in hepatic insulin signaling. Conversely, whole body glucose uptake as well as insulin signaling in skeletal muscle were unaltered, supporting that peripheral tissues remained insulin sensitive. In the liver, steatosis and insulin resistance were associated with local inflammatory changes. In control livers, as previously reported by others (27), few F4/80-positive hepatic macrophages coexpressed CD68 but all were CD11c negative. After 3 days of HFD, F4/80-positive cells appeared enlarged and the proportion of F4/80 and CD68 double positive cells increased together with upregulation of mRNA expression of macrophage-specific markers (TLR4, CD14, and TNF), whereas markers of alternative activation (35) remained unchanged (not shown). This supports the proinflammatory activation of resident hepatic macrophages (6, 57).

Table 3. *Effect of liposome-encapsulated clodronate on morphological, hepatic, and metabolic changes induced by a 3-day HFD*

	HFD	PBS + HFD	CLO + HFD
Body weight gain, g	2.4±0.9	3.4±0.7	2.1±1.2
Epididymal adipose tissue weight/body weight, %	1.3±0.1	1.3±0.2	1.0±0.1*
Liver weight/ body weight, %	5.7±0.4	5.8±0.2	6.1±0.5
Hepatic lipid content, mg/100 mg liver	9.3±2.8	11.7±4.7	11.6±4.0
Blood glucose, mg/dl	133.8±21.1	134.9±15.9	138.1±17.6
Serum insulin, μg/l	1.4±1.5	1.2±1.2	1.5±0.8

Results are expressed as mean ± SD (n = 6–8 per group) for mice fed a HFD for 3 days preceded by an intravenous injection of liposome-encapsulated PBS (PBS + HFD) or clodronate (CLO + HFD). *$P < 0.001$ in CLO + HFD vs. HFD or PBS + HFD.

In contrast with long-term exposure to high-fat diet in which hepatic steatosis is variable, if not absent (20, 21, 32), short-term high-fat diet yields reproducible steatosis (19, 43). Moreover, whereas KC activation is obvious in our 3-day model as also reported in human nonalcoholic steatohepatitis (25, 29, 36, 40), this is no longer found in the longer term regimen in rodents (9, 56, 59). By contrast, peripheral insulin resistance and recruitment of inflammatory cell in the adipose tissue, the hallmark of chronic obesity (28, 59), failed to be observed in our model. This implies that, in response to high-fat feeding, metabolic and inflammatory alterations occur first in the liver and secondarily in muscles and adipose tissues (peripheral tissues). We demonstrated here that selective ablation of KC significantly improved HFD-induced hepatic insulin resistance and alterations of hepatic insulin signaling, confirming a major role of KC in the initiating mechanism of HFD-induced hepatic insulin resistance, besides or irrespectively of inflammatory changes occurring in the adipose tissue.

Our results contrast with a recent publication (9) showing that, in mice exposed to a HFD for 16 wk, a single intraperitoneal injection of liposome-encapsulated clodronate decreased hepatic insulin sensitivity. Besides depleting the liver of F4/80-positive cells, intraperitoneal clodronate also induced significantly F4/80 mRNA in the adipose tissue (9). Such adipose tissue inflammation might be a confounding factor. We also performed intraperitoneal injections of clodronate in our short-term model. Contrasting with the selective depletion of KC via intravenous injections (liposomes do not cross vascular barriers), intraperitoneal clodronate affected ATM, as also reported by others (3), and upregulated fat MCP-1 and TNF implicated in macrophage recruitment (Supplemental Figure S1). Therefore, the significant upregulation of F4/80 in an already inflamed adipose tissue under chronic high-fat feeding reported by Clementi et al. (9) is consistent with a recruitment of macrophages following the clodronate-induced depletion. The effect of selective KC depletion on hepatic insulin sensitivity in a long-term HFD model remains to be evaluated.

Tissue fat accumulation is a cause of insulin resistance (31, 47). A dissociation between adiposity induced by high-fat feeding and insulin sensitivity, however, occurs when inflammatory pathways are inhibited (42, 48). Similarly, hepatic macrophage depletion prevented hepatic insulin resistance and alteration of hepatic insulin signaling without reducing hepatic steatosis elicited by high-fat feeding. Thus KC depletion also dissociates fat accumulation and hepatic insulin resistance. Therefore, hepatic accumulation of lipids or lipid metabolites known to alter insulin signaling in hepatocyte cultures (41) cannot be the sole cause of insulin resistance in vivo. Our results support that signals from local inflammatory cells acting downstream of IR concur to this effect, whether acting independently or amplifying those produced by the fat-loaded hepatocytes.

Intriguingly, KC depletion decreased adipose tissue weight while having no effect on body weight gain, liver weight, or degree of steatosis. Decreased adipose tissue could be the consequence of amelioration of hepatic inflammation and/or insulin sensitivity. Alternatively, although

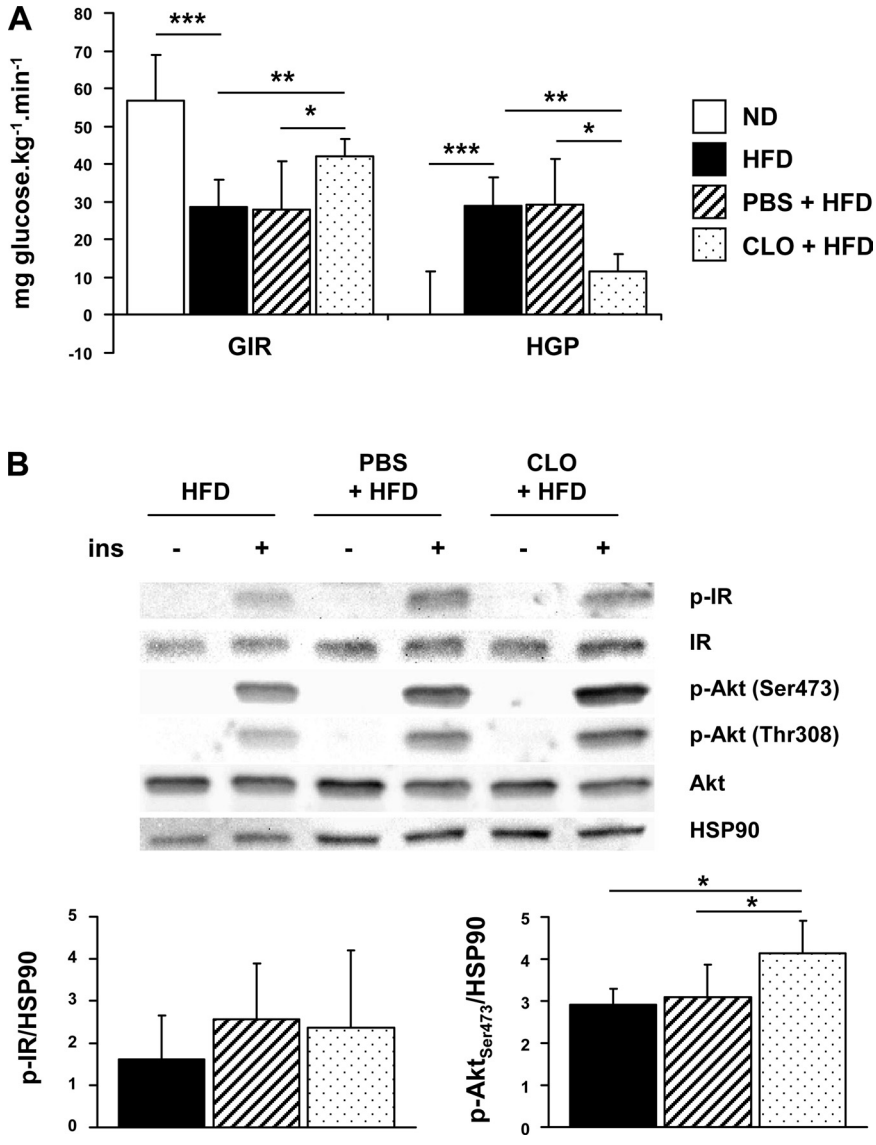

Fig. 5. Injection of liposome-encapsulated clodronate in HFD mice improves hepatic insulin sensitivity and signaling. *A*: GIR and HGP during hyperinsulinemic-euglycemic clamps. *B*: insulin signaling in liver of mice fed a 3-day HFD preceded or not by the iv injection of liposome-encapsulated PBS or clodronate (PBS + HFD or CLO + HFD, respectively). Graphs represent the quantification by densitometry analysis of the insulin receptor (IR) and Akt (ser473) phosphorylation upon insulin. Results are expressed as means ± SD ($n = 4$ per group). $^*P < 0.05$, $^{**}P < 0.01$, and $^{***}P < 0.001$.

not associated with decreased inflammatory signals, decreased adiposity may possibly contribute to amelioration of hepatic insulin sensitivity. Such phenomenon might also participate in the amelioration of insulin resistance observed upon gadolinium chloride treatment, which prevented HFD-induced weight gain (33). Further experiments are needed to address those issues.

Results presented here firmly establish that KC activation is a key mechanism in the induction of hepatic insulin resistance that develops upon high-fat diet feeding. Targeting KC to block this deleterious activation might therefore represent an effective strategy to prevent the development of hepatic insulin resistance. Further assessment of the role of KC in chronic obesity-induced metabolic alteration and deciphering the priming for KC activation, which could be triggered either by dietary factors or by products, whether cytokines or fatty acids, released by the gut, the adipose tissue or the fat-loaded hepatocytes, will be of major relevance for the understanding of diet-induced insulin resistance and for the development of new therapeutic approaches for the metabolic syndrome.

ACKNOWLEDGMENTS

The authors are grateful to Martine Petit, Valérie Lebrun, and Jorge Abarca-Quinones for expert technical assistance and to Prof. Hubert Piessevaux for help with statistical analysis. The monoclonal CD11b Ab developed by Timothy A. Springer was obtained from the Developmental Studies Hybridoma Bank developed under the auspices of the National Institute of Child Health and Human Development and maintained by the University of Iowa, Department of Biological Sciences, Iowa City, IA 52242.

GRANTS

This work was supported by Fonds National de la Recherche Scientifique (FNRS) grants (no. 3.4578.07 and F.45.08.08), la Direction de la Recherche Scientifique de la Communauté Française de Belgique (Action de Recherche Concertée grant, 05/10-328), University FSR grants 2007 and 2008 to I. A. Leclercq, grant "liver, virus and diabetes" from the Fondation St Luc to I. A. Leclercq and Y. Horsmans. I. A. Leclercq and P. D. Cani are FNRS research associates.

DISCLOSURES

The authors have no conflict of interest in relation to this work to disclose. The foundation Clodronate Liposomes (N. van Rooijen) is a nonprofit foundation related to the Department of Molecular Cell Biology of the Free University in Amsterdam, The Netherlands.

REFERENCES

1. **Adams LA, Lymp JF, St Sauver J, Sanderson SO, Lindor KD, Feldstein A, Angulo P.** The natural history of nonalcoholic fatty liver disease: a population-based cohort study. *Gastroenterology* 129: 113–121, 2005.
2. **Baffy G.** Kupffer cells in non-alcoholic fatty liver disease: the emerging view. *J Hepatol* 51: 212–223, 2009.
3. **Biewenga J, van der Ende MB, Krist LFG, Borst A, Ghufron M, Van Rooijen N.** Macrophage depletion in the rat after intraperitoneal administration of liposome-encapsulated clodronate: depletion kinetics and accelerated repopulation of peritoneal and omental macrophages by administration of Freund's adjuvant. *Cell Tissue Res* 280: 189–196, 1995.
4. **Burcelin R, Dolci W, Thorens B.** Portal glucose infusion in the mouse induces hypoglycemia: evidence that the hepatoportal glucose sensor stimulates glucose utilization. *Diabetes* 49: 1635–1642, 2000.
5. **Burcelin R, Uldry M, Foretz M, Perrin C, Dacosta A, Nenniger-Tosato M, Seydoux J, Cotecchia S, Thorens B.** Impaired glucose homeostasis in mice lacking the alpha(1b)-adrenergic receptor subtype. *J Biol Chem* 279: 1108–1115, 2004.
6. **Cai DS, Yuan MS, Frantz DF, Melendez PA, Hansen L, Lee J, Shoelson SE.** Local and systemic insulin resistance resulting from hepatic activation of IKK-beta and NF-kappa B. *Nat Med* 11: 183–190, 2005.
7. **Canbakan B, Senturk H, Tahan V, Hatemi I, Balci H, Toptas T, Sonsuz A, Velet M, Aydin S, Dirican A, Ozgulle S, Ozbay G.** Clinical, biochemical and histological correlations in a group of non-drinker subjects with non-alcoholic fatty liver disease. *Acta Gastroenterol Belg* 70: 277–284, 2007.
8. **Cani PD, Amar J, Iglesias MA, Poggi M, Knauf C, Bastelica D, Neyrinck AM, Fava F, Tuohy KM, Chabo C, Waget A, Delmee E, Cousin B, Sulpice T, Chamontin B, Ferrieres J, Tanti JF, Gibson GR, Casteilla L, Delzenne NM, Alessi MC, Burcelin R.** Metabolic endotoxemia initiates obesity and insulin resistance. *Diabetes* 56: 1761–1772, 2007.
9. **Clementi AH, Gaudy AM, Van Rooijen N, Pierce RH, Mooney RA.** Loss of Kupffer cells in diet-induced obesity is associated with increased hepatic steatosis, STAT3 signaling, and further decreases in insulin signaling. *Biochim Biophys Acta* 1792: 1062–1072, 2009.
10. **De Taeye BM, Novitskaya T, McGuinness OP, Gleaves L, Medda M, Covington JW, Vaughan DE.** Macrophage TNF-alpha contributes to insulin resistance and hepatic steatosis in diet-induced obesity. *Am J Physiol Endocrinol Metab* 293: E713–E725, 2007.
11. **Grimble RF.** Inflammatory status and insulin resistance. *Curr Opin Clin Nutr Metab Care* 5: 551–559, 2002.
12. **Hirosumi J, Tuncman G, Chang LF, Gorgun CZ, Uysal KT, Maeda K, Karin M, Hotamisligil GS.** A central role for JNK in obesity and insulin resistance. *Nature* 420: 333–336, 2002.
13. **Hundal RS, Petersen KF, Mayerson AB, Randhawa PS, Inzucchi S, Shoelson SE, Shulman GI.** Mechanism by which high-dose aspirin improves glucose metabolism in type 2 diabetes. *J Clin Invest* 109: 1321–1326, 2002.
14. **Jaskiewicz K, Rzepko R, Sledzinski Z.** Fibrogenesis in fatty liver associated with obesity and diabetes mellitus type 2. *Dig Dis Sci* 53: 785–788, 2008.
15. **Kanda H, Tateya S, Tamori Y, Kotani K, Hiasa KI, Kitazawa R, Kitazawa S, Miyachi H, Maeda S, Egashira K, Kasuga M.** MCP-1 contributes to macrophage infiltration into adipose tissue, insulin resistance, and hepatic steatosis in obesity. *J Clin Invest* 116: 1494–1505, 2006.
16. **Knauf C, Cani PD, Perrin C, Iglesias MA, Maury JF, Bernard E, Benhamed F, Gremeaux T, Drucker DJ, Kahn CR, Girard J, Tanti JF, Delzenne NM, Postic C, Burcelin R.** Brain glucagon-like peptide-1 increases insulin secretion and muscle insulin resistance to favor hepatic glycogen storage. *J Clin Invest* 115: 3554–3563, 2005.
17. **Kraegen EW, Clark PW, Jenkins AB, Daley EA, Chisholm DJ, Storlien LH.** Development of muscle insulin resistance after liver insulin resistance in high-fat fed rats. *Diabetes* 40: 1397–1403, 1991.
18. **Lanthier N, Horsmans Y, Leclercq IA.** The metabolic syndrome: how it may influence hepatic stellate cell activation and hepatic fibrosis. *Curr Opin Clin Nutr Metab Care* 12: 404–411, 2009.
19. **Lanthier N, Petit M, Lebrun V, Molendi O, Cani PD, Horsmans Y, Leclercq IA.** Exogenous steatosis and hepatic insulin resistance are early consequences of high fat feeding. *J Hepatol* 50: S262, 2009.
20. **Larter CZ, Yeh MM.** Animal models of NASH: getting both pathology and metabolic context right. *J Gastroenterol Hepatol* 23: 1635–1648, 2008.
21. **Larter CZ, Yeh MM, Williams J, Bell-Anderson KS, Farrell GC.** MCD-induced steatohepatitis is associated with hepatic adiponectin resistance and adipogenic transformation of hepatocytes. *J Hepatol* 49: 407–416, 2008.
22. **Leclercq IA, Farrell GC, Field J, Bell DR, Gonzalez FJ, Robertson GR.** CYP2E1 and CYP4A as microsomal catalysts of lipid peroxides in murine nonalcoholic steatohepatitis. *J Clin Invest* 105: 1067–1075, 2000.
23. **Leclercq IA, Lebrun VA, Starkel P, Horsmans YJ.** Intrahepatic insulin resistance in a murine model of steatohepatitis: effect of PPAR gamma agonist pioglitazone. *Lab Invest* 87: 56–65, 2007.
24. **Leenen PJM, Debruijn MFTR, Voerman JSA, Campbell PA, Vanewijk W.** Markers of mouse macrophage development detected by monoclonal antibodies. *J Immunol Methods* 174: 5–19, 1994.
25. **Lefkowitch JH, Haythe JH, Regent N.** Kupffer cell aggregation and perivenular distribution in steatohepatitis. *Mod Pathol* 15: 699–704, 2002.
26. **Livak KJ, Schmittgen TD.** Analysis of relative gene expression data using real-time quantitative PCR and the 2(T)(-Delta Delta C) method. *Methods* 25: 402–408, 2001.
27. **Lloyd CM, Phillips ARJ, Cooper GJS, Dunbar PR.** Three-colour fluorescence immunohistochemistry reveals the diversity of cells staining for macrophage markers in murine spleen and liver. *J Immunol Methods* 334: 70–81, 2008.
28. **Lumeng CN, DeYoung SM, Bodzin JL, Saltiel AR.** Increased inflammatory properties of adipose tissue macrophages recruited during diet-induced obesity. *Diabetes* 56: 16–23, 2007.
29. **Malaguarnera L, Di Rosa M, Zambito AM, dell'Ombra N, Nicoletti F, Malaguarnera M.** Chitotriosidase gene expression in Kupffer cells from patients with non-alcoholic fatty liver disease. *Gut* 55: 1313–1320, 2006.
30. **Marchesini G, Babini M.** Nonalcoholic fatty liver disease and the metabolic syndrome. *Minerva Cardioangiol* 54: 229–239, 2006.
31. **Marchesini G, Brizi M, Morselli-Labate AM, Bianchi G, Bugianesi E, McCullough AJ, Forlani G, Melchionda N.** Association of nonalcoholic fatty liver disease with insulin resistance. *Am J Med* 107: 450–455, 1999.
32. **Marsman HA, Al-Saady RL, Heger M, van Gulik TM.** How reproducible are rat steatosis models using high-fat diets? *J Hepatol* 51: 822–823, 2009.
33. **Neyrinck AM, Cani PD, Dewulf EM, De Backer F, Bindels LB, Delzenne NM.** Critical role of Kupffer cells in the management of diet-induced diabetes and obesity. *Biochem Biophys Res Commun* 385: 351–356, 2009.
34. **Nguyen MTA, Favelyukis S, Nguyen AK, Reichart D, Scott PA, Jenn A, Liu-Bryan R, Glass CK, Neels JG, Olefsky JM.** A subpopulation of macrophages infiltrates hypertrophic adipose tissue and is activated by free fatty acids via toll-like receptors 2 and 4 and JNK-dependent pathways. *J Biol Chem* 282: 35279–35292, 2007.
35. **Odegaard JI, Ricardo-Gonzalez RR, Eagle AR, Vats D, Morel CR, Goforth MH, Subramanian V, Mukundan L, Ferrante AW, Chawla A.** Alternative M2 activation of Kupffer cells by PPAR delta ameliorates obesity-induced insulin resistance. *Cell Metab* 7: 496–507, 2008.
36. **Park JW, Jeong G, Kim SJ, Kim MK, Park SM.** Predictors reflecting the pathological severity of non-alcoholic fatty liver disease: comprehensive study of clinical and immunohistochemical findings in younger Asian patients. *J Gastroenterol Hepatol* 22: 491–497, 2007.
37. **Patsouris D, Li PP, Thapar D, Chapman J, Olefsky JM, Neels JG.** Ablation of CD11c-positive cells normalizes insulin sensitivity in obese insulin resistant animals. *Cell Metab* 8: 301–309, 2008.
38. **Postic C, Girard J.** Contribution of de novo fatty acid synthesis to hepatic steatosis and insulin resistance: lessons from genetically engineered mice. *J Clin Invest* 118: 829–838, 2008.
39. **Rabinowitz SS, Gordon S.** Macrosialin, a macrophage-restricted membrane sialoprotein differentially glycosylated in response to inflammatory stimuli. *J Exp Med* 174: 827–836, 1991.
40. **Rensen SS, Slaats Y, Nijhuis J, Jans A, Bieghs V, Driessen A, Malle E, Greve JW, Buurman WA.** Increased hepatic myeloperoxidase activity in obese subjects with nonalcoholic steatohepatitis. *Am J Pathol* 175: 1473–1482, 2009.
41. **Ruddock MW, Stein A, Landaker E, Park J, Cooksey RC, McClain D, Patti ME.** Saturated fatty acids inhibit hepatic insulin action by modulating insulin receptor expression and post-receptor signalling. *J Biochem* 144: 599–607, 2008.

42. **Sabio G, Das M, Mora A, Zhang ZY, Jun JY, Ko HJ, Barrett T, Kim JK, Davis RJ.** A stress signaling pathway in adipose tissue regulates hepatic insulin resistance. *Science* 322: 1539–1543, 2008.
43. **Samuel VT, Liu ZX, Qu XQ, Elder BD, Bilz S, Befroy D, Romanelli AJ, Shulman GI.** Mechanism of hepatic insulin resistance in non-alcoholic fatty liver disease. *J Biol Chem* 279: 32345–32353, 2004.
44. **Schenk S, Saberi M, Olefsky JM.** Insulin sensitivity: modulation by nutrients and inflammation. *J Clin Invest* 118: 2992–3002, 2008.
45. **Schmidt MI, Duncan BB, Sharrett AR, Lindberg G, Savage PJ, Offenbacher S, Azambuja MI, Tracy RP, Heiss G.** Markers of inflammation and prediction of diabetes mellitus in adults (Atherosclerosis Risk in Communities study): a cohort study. *Lancet* 353: 1649–1652, 1999.
46. **Seppala-Lindroos A, Vehkavaara S, Hakkinen AM, Goto T, Westerbacka J, Sovijarvi A, Halavaara J, Yki-Jarvinen H.** Fat accumulation in the liver is associated with defects in insulin suppression of glucose production and serum free fatty acids independent of obesity in normal men. *J Clin Endocrinol Metab* 87: 3023–3028, 2002.
47. **Shoelson SE, Herrero L, Naaz A.** Obesity, inflammation, and insulin resistance. *Gastroenterology* 132: 2169–2180, 2007.
48. **Solinas G, Vilcu C, Neels JG, Bandyopadhyay GK, Luo JL, Naugler W, Grivennikov S, Wynshaw-Boris A, Scadeng M, Olefsky JM, Karin M.** JNK1 in hematopoietically derived cells contributes to diet-induced inflammation and insulin resistance without affecting obesity. *Cell Metab* 6: 386–397, 2007.
49. **Targher G, Bertolini L, Poli F, Rodella S, Scala L, Tessari R, Zenari L, Falezzal G.** Nonalcoholic fatty liver disease and risk of future cardiovascular events among type 2 diabetic patients. *Diabetes* 54: 3541–3546, 2005.
50. **Torres DM, Harrison SA.** Diagnosis and therapy of nonalcoholic steatohepatitis. *Gastroenterology* 134: 1682–1698, 2008.
51. **Van der Poorten D, Milner KL, Hui J, Hodge A, Trenell MI, Kench JG, London R, Peduto T, Chisholm DJ, George J.** Visceral fat: a key mediator of steatohepatitis in metabolic liver disease. *Hepatology* 48: 449–457, 2008.
52. **Van Hul NKM, Abarca-Quinones J, Sempoux C, Horsmans Y, Leclercq IA.** Relation between liver progenitor cell expansion and extracellular matrix deposition in a CDE-induced murine model of chronic liver injury. *Hepatology* 49: 1625–1635, 2009.
53. **Van Rooijen N, Sanders A.** Liposome-mediated depletion of macrophages: mechanism of action, preparation of liposomes and applications. *J Immunol Methods* 174: 83–93, 1994.
54. **Van Rooijen N, Sanders A, van den Berg TK.** Apoptosis of macrophages induced by liposome-mediated intracellular delivery of clodronate and propamidine. *J Immunol Methods* 193: 93–99, 1996.
55. **Weisberg SP, Hunter D, Huber R, Lemieux J, Slaymaker S, Vaddi K, Charo I, Leibel RL, Ferrante AW.** CCR2 modulates inflammatory and metabolic effects of high-fat feeding. *J Clin Invest* 116: 115–124, 2006.
56. **Weisberg SP, McCann D, Desai M, Rosenbaum M, Leibel RL, Ferrante AW.** Obesity is associated with macrophage accumulation in adipose tissue. *J Clin Invest* 112: 1796–1808, 2003.
57. **Wouters K, van Gorp PJ, Bieghs V, Gijbels MJ, Duimel H, Lutjohann D, Kerksiek A, van Kruchten R, Maeda N, Staels B, van Bilsen M, Shiri-Sverdlov R, Hofker MH.** Dietary cholesterol, rather than liver steatosis, leads to hepatic inflammation in hyperlipidemic mouse models of nonalcoholic steatohepatitis. *Hepatology* 48: 474–486, 2008.
58. **Wunderlich FT, Luedde T, Singer S, Schmidt-Supprian M, Baumgartl J, Schirmacher P, Pasparakis M, Bruening JC.** Hepatic NF-kappa B essential modulator deficiency prevents obesity-induced insulin resistance but synergizes with high-fat feeding in tumorigenesis. *Proc Natl Acad Sci USA* 105: 1297–1302, 2008.
59. **Xu HY, Barnes GT, Yang Q, Tan Q, Yang DS, Chou CJ, Sole J, Nichols A, Ross JS, Tartaglia LA, Chen H.** Chronic inflammation in fat plays a crucial role in the development of obesity-related insulin resistance. *J Clin Invest* 112: 1821–1830, 2003.
60. **Yamamoto T, Naito M, Moriyama H, Umezu H, Matsuo H, Kiwada H, Arakawa M.** Repopulation of murine Kupffer cells after intravenous administration of liposome-encapsulated dichloromethylene diphosphonate. *Am J Pathol* 149: 1271–1286, 1996.
61. **Yuan MS, Konstantopoulos N, Lee JS, Hansen L, Li ZW, Karin M, Shoelson SE.** Reversal of obesity- and diet-induced insulin resistance with salicylates or targeted disruption of IKK beta. *Science* 293: 1673–1677, 2001.